

SANDIA REPORT

SAND2010-5195

Unlimited Release

Printed August 2010

Uranium for hydrogen storage applications: A materials science perspective

Robert D. Kolasinski, Andrew D. Shugard, Craig R. Tewell, and Donald F. Cowgill

Prepared by
Sandia National Laboratories
Albuquerque, New Mexico 87185 and Livermore, California 94550

Sandia is a multiprogram laboratory operated by Sandia Corporation, a Lockheed Martin Company, for the United States Department of Energy's National Nuclear Security Administration under Contract DE-AC04-94AL85000.

Approved for public release; further dissemination unlimited.

Issued by Sandia National Laboratories, operated for the United States Department of Energy by Sandia Corporation.

NOTICE: This report was prepared as an account of work sponsored by an agency of the United States Government. Neither the United States Government, nor any agency thereof, nor any of their employees, nor any of their contractors, subcontractors, or their employees, make any warranty, express or implied, or assume any legal liability or responsibility for the accuracy, completeness, or usefulness of any information, apparatus, product, or process disclosed, or represent that its use would not infringe privately owned rights. Reference herein to any specific commercial product, process, or service by trade name, trademark, manufacturer, or otherwise, does not necessarily constitute or imply its endorsement, recommendation, or favoring by the United States Government, any agency thereof, or any of their contractors or subcontractors. The views and opinions expressed herein do not necessarily state or reflect those of the United States Government, any agency thereof, or any of their contractors.

Printed in the United States of America. This report has been reproduced directly from the best available copy.

Available to DOE and DOE contractors from
U.S. Department of Energy
Office of Scientific and Technical Information
P.O. Box 62
Oak Ridge, TN 37831

Telephone: (865) 576-8401
Facsimile: (865) 576-5728
E-Mail: reports@adonis.osti.gov
Online ordering: <http://www.osti.gov/bridge>

Available to the public from
U.S. Department of Commerce
National Technical Information Service
5285 Port Royal Rd.
Springfield, VA 22161

Telephone: (800) 553-6847
Facsimile: (703) 605-6900
E-Mail: orders@ntis.fedworld.gov
Online order: <http://www.ntis.gov/help/ordermethods.asp?loc=7-4-0#online>



SAND2010-5195
Unlimited Release
Printed August 2010

Uranium for hydrogen storage applications: A materials science perspective

Robert D. Kolasinski^(a), Andrew D. Shugard^(b), Craig Tewell^(a), and Donald F. Cowgill^(a)

^(a)Hydrogen and Metallurgical Science Department

^(b)Gas Transfer Systems Department

Sandia National Laboratories

P.O. Box 969

Livermore, California 94550-MS9161

Abstract

Under appropriate conditions, uranium will form a hydride phase when exposed to molecular hydrogen. This makes it quite valuable for a variety of applications within the nuclear industry, particularly as a storage medium for tritium. However, some aspects of the U+H system have been characterized much less extensively than other common metal hydrides (particularly Pd+H), likely due to radiological concerns associated with handling. To assess the present understanding, we review the existing literature database for the uranium hydride system in this report and identify gaps in the existing knowledge. Four major areas are emphasized: ³He release from uranium tritides, the effects of surface contamination on H uptake, the kinetics of the hydride phase formation, and the thermal desorption properties. Our review of these areas is then used to outline potential avenues of future research.

ACKNOWLEDGMENTS

We would like to express our appreciation to the Sandia/CA library staff, especially Sandra Lormand and Tiffany Vargas for their assistance in gathering the references needed to compile this report.

CONTENTS

Executive summary.....	1
Introduction.....	2
Phase diagram and P-c-T curves.....	3
³ He retention and bubble growth.....	5
Hydride formation rates from solid uranium metal.....	8
Decomposition kinetics.....	9
Surface oxide formation.....	10
Air-ingress accidents.....	12
Concluding remarks and summary of future research directions.....	12
List of figures.....	13
References.....	15

Uranium for hydrogen storage applications: A materials science perspective

I. Executive Summary

Under appropriate conditions, uranium will form a hydride phase when exposed to molecular hydrogen. This makes it quite valuable for a variety of applications within the nuclear industry, particularly as a storage medium for tritium. However, some aspects of the U+H system have been characterized much less extensively than other common metal hydrides (particularly Pd+H), perhaps due to radiological concerns associated with handling. To assess the present understanding, we review the existing literature database for the uranium hydride system in this report and identify gaps in the existing knowledge. Major areas emphasized include ^3He release from uranium tritides, the effects of surface contamination on H uptake, the rate of hydride phase formation, and thermal desorption of H and ^3He . Our review of these areas is then used to outline potential avenues of future research.

We have found the database of experiments which characterize ^3He release from uranium tritide to be rather sparse. The available laboratory studies suggest that for a period after the initial tritide formation, the uranium retains nearly 100% of the ^3He . After this point, release rate rises sharply, and eventually approaches the generation rate. The onset of this rapid release occurs at different times after the initial tritide formation, and the exact cause of the variation is not yet clear. Thermal desorption measurements suggest that ^3He desorbs most readily at 800 °C shortly after the tritide is formed. The desorption temperature migrates to lower values as the material ages and the $^3\text{He}/\text{U}$ ratio increases.

The rate at which the hydride phase is formed has received considerable attention, perhaps due to its relevance to uranium metal corrosion. From the perspective of hydrogen storage, such information is useful for describing the initial loading of the uranium bed and less relevant afterward. Several different models have been proposed to describe the hydride formation, although each appears to accurately reproduce the experimental data only under limited conditions.

The formation of an oxide on uranium surfaces has been studied rather extensively. There appears to be very little (if any) barrier to adsorbing oxygen-containing species on clean uranium surfaces. This has been shown to be true even during high-purity hydrogen exposure, where uranium was found to adsorb even trace amounts of contaminants. Thus, hydrogen absorption into uranium presents a very effective method of gas purification. Under most conditions it is reasonable to expect that uranium surfaces will include an oxide layer. Several researchers have noticed changes in the surface kinetics as the oxide coverage/thickness increased. Nevertheless, hydrogen can still apparently diffuse through the oxide (perhaps in molecular form) and into the bulk material. Heating tends to induce the formation of an oxygen-deficient oxide layer.

Finally, it has been established that rapidly exposing uranium to oxygen (as in the case of an air-ingress accident) releases a great deal of thermal energy. This pyrophoric nature of uranium presents a safety concern, as the heating of the hydride may result in the release of a large amount of hydrogen, as well as thermal energy. The available studies on this topic suggest that proper thermal design of the uranium bed can, to a large extent, minimize the hazards of a sudden oxygen leak into the system.

II. Introduction

The ability to store hydrogen in a compact manner is crucial for many scientific and industrial applications. Reacting hydrogen gas with metals to form a hydride phase is a particularly attractive and practical method of gas purification and compact storage. For this reason metal hydrides have been investigated extensively over the past several decades, and a number of well-suited materials have been identified. (Dantzer provides a critical review of the existing technology in Ref. [1].) While lightweight materials are desirable for portable storage applications in the transportation industry; the requirements are less stringent for stationary storage systems.

Under appropriate conditions, uranium will form a hydride (UH_3) phase when exposed to $\text{H}_2(\text{g})$ and, as a result, has found continued use in the nuclear industry for the past 40 years for tritium storage [2], [3]. The difficulties associated with handling uranium hydride (particularly its radioactivity and high pyrophoricity with oxygen) suggest the following question: What advantages does using uranium offer, particularly when so many alternative hydride materials are available? Uranium in fact satisfies several important criteria which make it attractive for tritium storage. First, uranium-hydride has a low equilibrium pressure (< 0.1 Pa) at room temperature, thereby minimizing tritium loss when the manifolds of the storage system are purged. (This has the additional practical benefit of decreasing the load placed on the tritium waste management system.) The stored tritium can be recovered fairly quickly by heating it up to a convenient temperature of 400-450 °C, for which it produces a supply pressure in excess of 10^5 Pa. This temperature is low enough so that loss of tritium by permeation through containment systems is not an overriding concern. Furthermore, the equilibrium pressure varies very slowly with composition in the plateau region of the P - c - T curves. In addition to these favorable thermodynamic properties, the kinetics of hydrogen uptake and release appear to be rather tolerant to trace amounts of impurities within the exposed hydrogen gas. Rather than immediately poisoning the surface the oxide tends to diffuse into the bulk upon heating, and the deterioration of kinetics of hydrogen uptake and release are gradual.

Despite the aforementioned advantages, a number of challenges to using uranium in practical storage systems exist. First, uranium hydride tends to break up into fine sub-micron sized particles, thereby requiring a containment system for the fragments. Even with such countermeasures in place, the fragments can still migrate to other components in the same feed system containing the U-beds. Exhaust of the U particles from the system also presents an inhalation hazard. As discussed previously, high reactivity with oxygen also presents a safety concern. For example, during a recent incident at Argonne National Laboratory –West, uranium corrosion products containing a mixture of UO_{2+x} and UH_3 ignited unexpectedly during a transfer of this material between storage containers. (The fire eventually extinguished itself; further details are provided in Ref [4].) Finally, because uranium is also radioactive and is generally classified as a controlled nuclear material, handling and accountability measures applied to uranium beds can be rather complex.

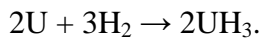
The drawbacks mentioned above have raised the concerns of many researchers, particularly in the nuclear fusion community where large scale tritium storage is needed. In ITER, a large international magnetic fusion experiment presently under construction, 3 kg of tritium will be stored on site in approximately 50 hydride beds. An inter-metallic material, ZrCo, has been

proposed as the best alternative for storage applications because of it has similar thermodynamic properties as U [5]. ZrCo has low reactivity with oxygen and nitrogen and avoids any radiological concerns. In addition, the volumetric expansion, $(V_{\text{hydride}} - V_{\text{metal}})/V_{\text{metal}}$, of ZrCo is 0.2, a value much less severe than in U (typically 0.75; see work by Shuai in Ref. [6] for more details on the amount of swelling as a function of hydriding cycle.) Nevertheless, while the thermodynamic properties of ZrCo are favorable for storing tritium, its uptake/release rate and equilibrium pressure at room temperature are inferior to those of U. Hence in an emergency situation where rapid recovery of tritium is crucial, uranium may be viewed as a superior choice.

This review focuses on evaluating the present experimental and modeling database relevant to the storage of hydrogen in uranium. In previous work, Manchester [7] used available experimental data to assemble the phase diagram and pressure-composition isotherms for uranium-hydrogen system. Since these results have been well established, they are mentioned briefly at the beginning of this report, and other aspects of the U+H system are reviewed thereafter more thoroughly. The remaining literature loosely fits into four subdivisions. First, we examine the long-term effects of tritium storage, particularly retention of ^3He generated from tritium decay. The details of the hydride phase are discussed, including the nucleation and growth kinetics, as well as surface morphology. We also present the current understanding of how oxide forms on the clean U surface and its impact on H uptake. The chemical behavior of uranium when exposed to oxygen (in particular the effects of oxides on the hydride kinetics) are discussed in detail. This review concludes with a brief treatment of the pyrophoric nature of uranium, particularly the effect of air-ingress accidents.

III. Phase diagram and P - c - T curves

The reaction for uranium hydride formation is given by the well known equation:



The U+H equilibrium phase diagram has been reviewed extensively by Manchester [7], and we summarize the major findings here. Five different phases of U+H have been found under varying conditions, although the present review will focus on what is referred to as the “ ϵ -phase.” Generally indicated as simply as “ UH_3 ”, this phase occurs for H at. % > 75 for temperatures at least up to 1100 °C. The crystal structure of UH_3 hydride is cubic, with a lattice constant of $a=6.625\pm 0.003$ Å at room temperature [8]. This suggests a rather large volume expansion compared with the orthorhombic crystal structure of pure uranium metal at room temperature, with lattice constants $a=2.854$ Å, $b=5.870$ Å, and $c=4.955$ Å. In practice, a 75% expansion by volume is observed experimentally.

The pressure-composition isotherms have been explored by numerous investigators, and much of this data has been reviewed by Manchester [7] and Penzhorn [9]. The plateau pressure and temperature generally follow the well-known relationship $\log P = -A/T + B$. Manchester suggests the data of Mallet [10] is the most authoritative, which gives $\log P$ (Pa) = $-4590/T$ (K) + 11.52. A plot of previously published values compiled by Penzhorn (data contained in Table 3 therein) is shown in Fig. 1. A hysteresis was typically noted between absorption and desorption of H, and these cases are plotted separately in panels (a) and (b), respectively. The isotope

dependence of the plateau pressure does not appear to be especially strong. Results from Tanabe [11] suggest an isotope separation factor $\alpha=[D/H]_g/[D/H]_s=1.3$ with the dissociation pressure of UD_3 higher than UH_3 by a factor of 2 at 400 °C. However, this appears to be a rather minor effect compared with the variation in absolute values observed between different laboratories. Performing a least-squares fit to the existing literature database provides a relationship that is in good agreement with results of Mallet:

$$\log P \text{ (Pa)} = -4701/T \text{ (K)} + 11.81 \text{ (absorption)}$$

$$\log P \text{ (Pa)} = -4216/T \text{ (K)} + 11.08 \text{ (desorption)}$$

The pressure-composition isotherms depicted in Fig. 2 were also assembled by Manchester using data from Libowitz and Gibb [12]. Since the isotherms are very flat for the temperature range of interest here, only the high atomic ratio ($X=H/U$) region is shown in Fig. 2. The full P-c-T curves are depicted in Fig. 3, again using data from Libowitz.

Of interest are also the basic thermodynamic properties of the U+H system. The available data were reviewed by Manchester. The reaction of U with H is exothermic, and the calorimetric data of Abraham [13] is suggested as the authoritative reference for enthalpies and entropies of formation (values below given for 25 °C):

$$-\Delta_f H^{(UH)_3} = -127.0 \text{ kJ}/0.5 \text{ mol H}_2$$

$$-\Delta_f H^{(UD)_3} = -129.8 \text{ kJ}/0.5 \text{ mol D}_2$$

$$-\Delta_f H^{(UT)_3} = -130.3 \text{ kJ}/0.5 \text{ mol T}_2$$

Based on available data sets, the entropy of formation at 25 °C was calculated by Manchester to be:

$$\Delta_f S^\circ = -182 \text{ J/K}\cdot 0.5 \text{ mol H}_2$$

Further thermodynamic data may be found in Manchester's review, or in JANAF tables. Basic properties of uranium and uranium hydride are summarized in Tables 1 and 2.

Table 1: Basic properties of uranium and uranium hydride

	U	UH ₃
Density (theoretical), ρ	19.05 g/cm ³	10.92 g/cm ³ [14] (meas. for UH ₃)
Crystal structure	orthorhombic	cubic
Lattice constants	$a=2.854 \text{ \AA}$ $b=5.870 \text{ \AA}$ $c=4.955 \text{ \AA}$ $\alpha=\beta=\gamma=90^\circ$	$a=6.625\pm 0.003 \text{ \AA}$ (meas. for UT ₃ [8]) $\alpha=\beta=\gamma=90^\circ$

Storage capacity of hydride, N_H	-	8.2×10^{22} at./cm ³
Weight percent of hydrogen in hydride, w_H	-	1.25%
Volume expansion of hydride $(V_{hydride} - V_{metal})/V_{metal}$	-	0.75

Table 2: Effective thermal conductivity of un-oxidized uranium metal powder based on measurements by Swift [15]. Uranium hydride conductivities based on measurements and theoretical calculations by Erikson [16].

	Gas	K [W/m ² K]
U (solid)	N/A	24.7
U (powder)	Ar	0.255
	N ₂	0.343
	He	1.34
U (hydride)	N/A	1-2

IV. ³He retention and bubble growth

A. Characterization of ³He bubbles using Nuclear Magnetic Resonance Spectroscopy

The decay of tritium to form ³He presents complications which are unique to metal tritide systems. Given a half-life of 12.3 years, the ³He/T ratio can be expected to increase by 1.55×10^{-4} per day assuming 100% retention. Despite the expected low solubility for ³He in most metals, prior work has shown that appreciable quantities may reside within metals for prolonged periods after T loading. (Ratios as high as 0.1 He/ T have been reported [17] after 1600 days.) Investigating these effects experimentally in UT₃ presents challenges due to radiological contamination concerns associated with handling tritium (thereby requiring specialized microscopy facilities to observe microstructure changes induced by the ³He.) Furthermore, the decay time required to produce the ³He makes generating samples a slow process. Nevertheless, a number of valuable studies have contributed to the present understanding of ³He in uranium.

Given the rather high He/T ratios which can be found in U, the question arises as to whether this He is contained at interstitial lattice sites or within small bubbles in the material. A rather definitive answer to this problem was provided by Bowman through a series of nuclear

magnetic resonance (NMR) spectroscopy studies [17, 18], which showed ^3He was contained in microscopic bubbles $<500 \text{ \AA}$ in dia. NMR is one of the few techniques which can provide insight into the formation and growth of ^3He bubbles. Further details may be found in Ref. [19].

The NMR measurements of Bowman provide qualitative insight into how ^3He is retained and released from the material. After the initial formation of the tritide, ^3He bubbles are nucleated soon afterward. Assuming the diffusivity He in U is sufficiently high, the ^3He formed by tritium decay will quickly move through the material until it encounters a bubble. At this point, it precipitates out of solution, the continuous process of trapping at these locations induces bubble growth. The ^3He inventory within the bubbles is released due to mechanical failure (“rupture”) of the bubble wall. Bowman’s study focuses on the measurement techniques required to characterize He in U. The fraction of He retained in the material is likely the most important result for the purposes of this review. Despite these interesting results, subsequent NMR studies of the U+H system have been rather sparse. (Later work by Barash [20] examined the magnetic properties of UH_3 but did not address ^3He bubble growth.) One might envision that radiological concerns associated with handling U have discouraged further work in this area. X-ray diffraction studies by Ao and co-workers [21] also show considerable lattice distortion in UT_3 that has aged 420 days. As depicted in Fig. 4, such changes were not observed after a similar period of time for UH_3 . These measurements seem to support Bowman’s conclusions regarding bubble growth, and suggest that ^3He accumulation in the material severely distorts the crystal lattice.

B. Thermal desorption of ^3He

The production of ^3He by decaying tritium also presents some complications for thermal desorption of UT_3 . If released during the desorption process, ^3He is a source of contamination for the released tritium. Because this issue arises over long-term storage of UT_3 , the sparseness of experimental results addressing this topic is not particularly surprising. Relevant studies were executed by Malinowski and Coronado [22], who characterized ^3He release from several fully stoichiometric UT_3 samples over a 1200 day period, and also by Bowman [17] in the previously described NMR studies. Malinowski et al. found that the ^3He release was minimal ($< 2\%$) until 280 days of storage had elapsed. After this time, the quantity released increased rapidly, approaching the rate generated by decay after 1000 days. Bowman reports ^3He retained (rather than amount released), although the interpretation of such data is practically the same. Bowman’s data show that very little ^3He is released until 700 days, after which the ratio of ^3He to T asymptotes to a level of $^3\text{He}/\text{T}=0.12\pm 0.01$ at 1200 days. Both data sets are plotted in Fig. 5.

Qualitatively, the behavior observed by Malinowski et al. and Bowman appears similar, although the onset of the rapid ^3He release occurs at different times. It is interesting to note that Malinowski used an overpressure of 800 torr of T to replenish losses encountered through decay, whereas Bowman had backfilled with Ar. It is possible that the added tritium reservoir promoted more rapid bubble growth and the earlier release observed in Malinowski’s case. Another possibility is that microstructural differences in the uranium tritide accounted for the variation in the onset of ^3He release. However, specific surface area measurements using the Brunauer-Emmett-Teller (BET) method provide some indication of particle size; Bowman reported a BET surface area range of $0.40\text{-}0.85 \text{ m}^2/\text{g}$, whereas Malinowski reported similar value of $0.6 \text{ m}^2/\text{g}$.

Both of these values are reasonably consistent, and unfortunately, neither study contained microscopy results which included a characterization of particle sizes.

It is also worthwhile to consider at what temperatures ^3He would desorb most rapidly from U. Berezko [23] investigated this in a series of temperature programmed desorption experiments for UT_3 samples aged between 1.6-13.9 yrs. The desorbed gases were characterized with a mass spectrometer. In Fig. 6, desorption spectra for $m/q=3$ (corresponding to ^3He) are depicted for samples of various ages. The thermal ramp can affect the location of desorption peak positions; in this study a constant rate of $35\text{ }^\circ\text{C}/\text{min}$ was used. For relatively new samples (<2.2 yrs after hydride formation) the ^3He desorbs rather abruptly at $800\text{ }^\circ\text{C}$. As the hydride ages (and the $^3\text{He}/\text{U}$ increases) this temperature migrates to lower values. After 13.9 yrs the ^3He is observed to desorb at $400\text{ }^\circ\text{C}$. At this lower temperature, the desorption peak is much broader.

Care must be taken when interpreting the above results because ^3He corresponds to a mass/charge ratio of $m/q=3$, which is also true for HD , H_3^+ , and T^+ . Hence, it may not be possible to unambiguously determine the composition of the gases desorbed from the hydride when relying on mass spectrometry alone. To circumvent this problem, Berezko exposes the uranium to a mixture of T ($\approx 30\%$) and D prior to thermal desorption. One would expect the D and T gases to behave in a similar manner. This is demonstrated by the desorption spectra shown in Fig. 7. In this case, for samples aged by 1.6 and 2.2 yrs, the desorption patterns for $m/q=4$ and $m/q=6$ behave quite similarly, with peak values at $400\text{ }^\circ\text{C}$. The $m/q=3$ peak behaves much differently, suggesting that the $m/q=3$ peak is mainly due to ^3He . This argument is buttressed by the argument that one would expect T to recombine at the U surface and desorb as T_2 .

C. *Future avenues of research*

The above mentioned results are of course quite valuable to our present understanding of ^3He retention in uranium hydride. However, there are some obvious gaps in the existing literature. One topic which readily comes to mind is the effect that uranium hydride particle size has on the accelerated release of ^3He . As previously mentioned, the studies of Malinowski and Bowman include BET measurements (which give an average particle size) but no microscopy was performed. The effect of hydride temperature and stoichiometry on ^3He retention has also yet to be fully investigated. While Bowman's results provide much insight into bubble growth, the results are over 30 years old at this point. It seems reasonable to assume that the significant advances in NMR spectroscopy since that time could certainly yield much more insight.

While investigating these issues may at first seem to be an attractive possibility, one obvious difficulty is the aforementioned problem of accumulating ^3He in the hydride material. While the half-life of T is not especially long, many of the effects of ^3He accumulation require years to become apparent. The question then arises as to whether one can accelerate this process. One possibility is ^3He implantation using a high energy ($> 100\text{ keV}$) ion accelerator. Presumably the He would accumulate and form bubbles at vacancies created by the implantation process, and as a starting point one could easily envision implanting into thin U foils. However, examining the effect of such implantation on uranium hydride could be much more difficult, as this would require implanting into a powder. Techniques for performing such implantations have been previously developed by Ensinger [24].

Another avenue of further work would be to simulate the growth of ^3He bubbles using available computational models. Such a technique has been previously developed by Cowgill, using an approach which unifies aspects of a variety of different models into a single package. Further details on this approach may be found in Ref. [25].

V. Hydride formation rates from solid uranium metal

The amount of hydride formed as a function of time can be determined by (among other methods) pressure measurements during H_2 uptake or by thermogravimetric analysis. Such techniques have been employed by a number of investigators in an attempt to provide a data set which would allow a hydriding model to be developed. To address this point, Powell et al. [26] performed measurements using a series of samples machined from bulk uranium, and compared the results with the existing literature database. The authors also evaluated models proposed by Kirkpatrick [27], Bloch [28], and Wicke [29] which described the hydriding kinetics. The results of this review are described in Ref. [26], and are summarized here.

From a qualitative perspective, the reaction begins at the outer surface of the bulk metal, forming hydride islands which grow in size until the entire surface is covered. The reaction interface then propagates through the material. The outer hydride film, owing to the large volume expansion, breaks away from the surface. For planar specimens, this boundary is well defined, as illustrated by the SEM cross-section of a H-exposed U foil in Fig. 8 (obtained from Bloch's study [28].) Case (a) shows the foil prior to H_2 exposure, whereas case (b) shows the foil afterward. The rate of progression of the reaction front through the material can of course be assessed through such images or more conveniently through gas balance calculations (as in Powell's experiments.)

The hot stage microscope measurements of Bloch [30] reveal the initial stages of hydride formation. This phase is decidedly more complex and difficult to model compared with the reaction front propagation through the material. Fig. 9 illustrates the process qualitatively, showing surface images of U metal foils obtained at varying points during the hydriding process. Initially, small hydride spots form within grain boundaries as shown in (a). For the conditions of Bloch's experiments, these spots grow to approximately $10\ \mu\text{m}$ in diameter and maintain a constant size for some time thereafter. (Bloch refers to this as the "pre-induction" stage, shown in panels (b) and (c) of Fig. 9.) After this point, the hydride islands grow at a nearly linear rate. The islands continue to grow at this rate until they begin to overlap, as illustrated in Fig. 10(a-c). Eventually the islands cover the entire surface and the outer hydride film begins to crack and break apart (shown in panels d-f).

The initial rate of hydride formation was also examined in Powell's study, where a high speed data acquisition system was used to monitor the hydriding rate of 3.18 mm dia. uranium rods. After prior exposure in a hydrogen atmosphere, the rods were annealed for a period of 3×10^5 s at $250\ ^\circ\text{C}$. Hydriding rate data compiled from four different exposures of a single specimen to H_2 are shown in Fig. 11. It seems reasonable that Powell's data could be interpreted using the qualitative observations of Bloch described above. An initial rapid increase in the hydride formation rate is followed by a short constant-rate period. It seems reasonable that this

could be the pre-induction stage described above. The hydride formation rate subsequently increases rapidly, which Powell attributes to “exfoliation” of the hydride film.

Pretreatment of the sample materials (particularly annealing) and purification of the H gas appear to be crucial to obtaining reproducible measurements. This need was initially recognized by Condon, and later by Powell who found the reaction rate to be particularly sensitive to oxygen contamination and residual stresses in the material. In his review, Powell points out that Bloch did not take these precautions, and suggests that those results are affected by oxide formation (and may therefore be suspect.) Bloch later performed a detailed study addressing the effects of thermal annealing, as discussed in Ref. [31].

Quantitative predictions of hydride formation rates, on the other hand, are a bit more challenging to achieve. As previously mentioned, several different research groups developed models which describe specific aspects of the experimental database, but do not describe all behavior. Early experimental and theoretical work by Condon [32] [33], paved the way for a more sophisticated treatment by Kirkpatrick [27]. To evaluate the range of validity of each of these models, Powell measured the hydriding rate of uranium foils and rods over a wide range of conditions. His data are shown in Fig. 12. Powell noted that hydrogen isotope effects did not appear to be important in terms of the reaction rate. In his work on the subject, Powell provides a detailed comparison of the available hydride models, and evaluates their predictive capabilities. We therefore refer the reader to Powell’s analysis in Ref. [26] for an in-depth discussion of the advantages and disadvantages of each approach.

VI. Decomposition Kinetics

The P - c - T curves described in Sect. III were obtained at near-equilibrium conditions where the stored hydrogen was evolved in a vacuum environment. However, in many practical applications the rate at which hydrogen can be delivered from the storage bed is crucial. In many cases, de-hydriding takes place in an environment which includes a hydrogen overpressure. Decomposition of UH_3 in the temperature range of 390-500 °C was investigated by Linder, as described in Ref. [34].

Linder’s experiments were performed using a U storage bed attached to a manifold which included a mass flow controller. This controller regulated the flow of H_2 evolved from the U bed into a series of calibrated volumes. The amount of gas collected was calculated based on the pressure accumulated in these volumes. With this apparatus, Linder was able to characterize the “dynamic” P - c - T curves, which can be represented using the same Van’t Hoff formulation applied to the equilibrium systems. With the evolved gas flow rate limited to $0.035 \text{ H/U min}^{-1}$, Linder calculated the following fit to the dynamic P - c - T data:

$$\log P_0 \text{ (Pa)} = -4700/T \text{ (K)} + 11.26$$

A number of models were considered for the decomposition rate. Initially Linder observed the rate of decomposition was linear, indicating the process could possibly be modeled with zero-order kinetics. However, a model based on the advance of the metal-hydride phase boundary provides better agreement over the entire reaction. For this case, the relationship for the best decomposition kinetics is given by

$$\alpha = 1 - \{1 - k(P, T)\}^3$$

where α is the fraction of hydride which has decomposed, and P and T indicate pressure and temperature, respectively. The rate constant $k(P, T)$ exhibits an Arrhenius behavior according to the following relationship:

$$k(P, T) = a \ln\left(\frac{P_0}{P}\right) e^{-E_a/RT}$$

where the decomposition activation energy is $E_a=18.9\pm 1.8$ kcal/mol, $a=1860$ min⁻¹, and P_0 is determined as described above.

While Linder's more data highlights many important processes needed to model rapid desorption of hydrogen from a uranium bed, more data over a wider range of temperatures, pressures, and flow rates would certainly be welcome.

VII. Surface oxide formation

A. Initial stages of formation

Bloch and co-workers investigated the kinetics of oxide formation on U surfaces [35]. In this series of experiments, x-ray photoelectron spectroscopy (XPS) and Auger electron spectroscopy (AES) were used to examine adsorption rates of oxidation of U surfaces in UHV conditions. The uranium surfaces were prepared by sputter cleaning with a low energy Ar⁺ source and were subsequently exposed to atmospheres of high purity (99.999%) O₂, H₂, and CO₂. (With a base pressure of 2×10^{-8} Pa, about 1 hr would be needed to accumulate a monolayer of contaminant species from the background alone.) The authors were not able to provide calibrated values of surface coverage, and only the ratio of the Auger signals for O (oxide) and U are presented.

Even under UHV conditions, Bloch et al. observed the formation of an oxide layer on a clean U surface almost immediately, with the rate dramatically increasing after 1 hr. As one would anticipate, this rate is accelerated by introducing an oxidizing atmosphere, even at relatively low pressures ($1.5\text{-}2\times 10^{-6}$ Pa). The rate of oxide formation was highest for O₂(g) exposure, followed by CO₂(g) exposure. While one would not anticipate that exposing the surface to pure H₂(g) would initiate the formation of an oxide layer, the authors found this type of atmosphere caused a slight increase in the growth rate compared to the UHV case. One could reason that this is due mainly to impurity species within the H₂ supply. If true, this would indicate that even minute amounts of O₂ or CO₂ will accumulate on the surface rather rapidly.

The Auger peak positions corresponding to chemisorbed O and oxide occur at slightly different energies. Observations made of the peak position immediately before and after sputter cleaning suggested that oxide formation is immediately preceded by chemisorption of O₂. (The chemisorbed O₂ dominates for 20 min after sputter cleaning under UHV conditions.) Follow-up work by Wang et al. [36] and Balooch and Hamza confirmed the findings of previous studies which showed that an oxide free surface was nearly impossible to maintain, even under UHV conditions.

XPS depth profiling can provide a wealth of information on the distribution of the oxide with respect to the surface. In the case of Wang's study, signals from UO_2 , UH_3 , and U were monitored as a function of depth. The outer surface was found to be dominated by UO_2 , with an atomic concentration initially in excess of 80%. This concentration diminished with depth, and an intermediate UH_3 layer was detected before the bulk material was reached. With this in mind, Wang proposed the configuration shown in Fig. 13. Wang suggests that the first stage in the formation of the surface layer involves dissociative adsorption of $\text{H}_2(\text{g})$ on the clean U surface. Trace impurities from the H_2 atmosphere (particularly O_2 and H_2O) will immediately begin to adsorb on the surface eventually forming a UO_2 layer. With continued exposure, the H_2 eventually diffuses through the oxide layer (although it is not clear from the work of Wang whether it diffuses as a atomic or molecular H) and forms a hydride layer at the boundary of the bulk material and oxide.

Based on the results described in Ref. [35], maintaining a clean U surface will be nearly impossible, even under favorable conditions. A question which naturally arises from this analysis is: how will minute amounts of impurities affect the uptake of H_2 within material? The molecular beam studies of Balooch and Hamza were aimed at addressing this issue [37]. The sticking probability of H_2 on a clean U surface was found to be 3×10^{-2} ; this probability was decreased by two orders of magnitude if the surface was not sputter cleaned prior to exposure.

B. Heat-induced modifications to the oxide layer

Although O has a rather small diffusivity in U at room temperature, it is possible to change the oxide distribution within the surface by thermal annealing. This was demonstrated by Swissa [38] through a series of AES studies aimed at characterizing the native oxide layer and oxides produced by deliberate exposure to O. To determine the thickness and composition of the native oxide, Swissa performed AES profiling on U samples prepared using different techniques. As illustrated in Figs. 14a and b, cleaning an as-received U sample with 50% HNO_3 (14b) reduces the carbon content in the sample material substantially. The most reproducible cleaning process included electrolytically polishing the surface, as illustrated in Fig. 14(c). For a practical uranium storage system, the initial state of the native oxide on the metal likely is not a significant factor. However, since much of the experimental work reviewed in this report was performed using U foils, Swissa's analysis is still quite valuable for critically evaluating the published literature. As an example, in prior work by Powell [26], the amount of oxide initially on a U surface prior to exposure to H strongly affected the hydride formation rate.

Swissa used similar AES profiling to measure the redistribution of oxide upon heating. An AES profile before and after heat treatment is shown in Fig. 15. The data was obtained for a sample that was profiled after having been annealed in a separate chamber at 600°C after 40 min. Therefore, the surface was exposed to atmosphere after the annealing process during the transfer to the AES system. In Fig. 15, the region labeled "1" indicates the portion of the profile pertaining to the native oxide. (Because of air exposure, the native oxide is evident for both samples, having formed on top of the clean metal surface.) Region "2" indicates a uranium-enriched layer just beneath the native oxide, and region "3" indicates a second oxide layer further into the surface. The mechanism for the formation of the uranium-enriched region was not clear from Swissa's experiments; several possibilities are mentioned in Ref. [38].

VIII. Air-ingress accidents

One concern associated with the use of uranium as a storage material is its pyrophoric nature. Initial cases of rapid exposure of small quantities of uranium (on the order of 1 mg) resulted in very high temperature excursions in preliminary tests performed at INL. This led researchers to suspect that a rapid accidental exposure of a uranium bed to air could lead to a large release of energy and evolution of tritium. The potential consequences were investigated by Longhurst and are described in Ref. [39].

In Longhurst's study, beds containing 5 g, 25 g, and 3 kg were considered at temperatures ranging between $298\text{ K} \leq T \leq 824\text{ K}$ for varying amounts of hydride ($0 \leq H/U \leq 1.5$). Each bed was attached to a manifold and loaded with a calibrated amount of deuterium or tritium gas. Various compositions of ingress gases were considered, including air, N_2 , O_2+He , O_2+Ar , and 20% $O_2+80\%$ N_2 mixtures. The larger 3 kg beds were mounted to a manifold which could monitor the amount of tritium evolved, as well as capturing the HT and HTO species on copper-oxide beds.

Surprisingly, Longhurst et al. found the thermal excursions caused by reaction with air were much less severe than anticipated. In particular, the observed temperature rise in all cases but one was less than $\Delta T \leq 35\text{ }^\circ\text{C}$. The lone exception occurred when a 3 kg bed was exposed rapidly to air, resulting in an excursion of $\Delta T = 175\text{ }^\circ\text{C}$. (This outlier performance was considered to be due to a faulty heating system on the bed in question.) Several mechanisms that might contribute to limiting the extent of the reaction were proposed. The first of these was the formation of a film of reaction products on the surface of the hydride, which seems to prevent the reaction from proceeding further. The presence of non-reacting gases already within the bed was also considered a contributing factor. Further details may be found in Ref. [39].

While Longhurst's results are encouraging, when handled outside of a well-designed containment system uranium hydride can still react violently with oxygen. As an example, Totemeier describes a recent event where UH_3 was being consolidated into a single container under a fume hood at Argonne National Laboratory – West in Ref. [4]. In one instance during transfer, the material began sparking causing the formation of flames. (Ejection of gas during the burning process made it impossible to extinguish the flames with standard fire-retardant. The fire eventually burned out on its own.) The specific ignition source could not be identified during post-mortem analysis, and as a precautionary measure all future transfers were recommended to be conducted in an inert environment, or first taking steps to passivate the surface.

IX. Concluding remarks and summary of future research directions

As we have previously discussed, uranium has many attributes which make it attractive as a tritium storage medium. Our findings indicate the technical information needed to design uranium for short-term hydrogen storage is sufficiently mature. Further work, however, is believed to be necessary to ensure reliable long-term storage of tritium. In this report we have reviewed some of the materials-science issues which could have implications for the long-term

use of uranium in practical tritium storage systems. Areas which merit further study are summarized below.

The PCT curves for uranium have been measured to sufficient accuracy for most practical hydrogen storage applications. From Manchester's review, more work could be done to better understand the phase diagram at low hydrogen concentrations; however, such information is not likely to be of much relevance for storage applications. Exchange experiments, similar to those conducted by Luo [40] for the Pd system would likely be quite valuable.

Generation of ^3He is a concern when storing T for long periods of time. The fraction retained within the hydride has been characterized in multiple studies, but the factors which affect the thermal stability of this ^3He and the onset of rapid release need to be determined. One obvious way to study these effects is by loading uranium beds with tritium and storing them. However, difficulties associated with using tritium and the length of time required to execute the experiments would limit the number of experiments that can be performed in practice. Implantation of high energy ^3He into U using an accelerator may be one possible method for investigating the effects mentioned above without using tritium. Another aspect of this problem which has not been addressed is the effect on microstructure of the uranium tritide. It is suspected that the lattice distortion induced by the presence of He may contribute to the decrepitation of the U tritide. With this in mind, a study to determine the nature of individual uranium tritide particles (crystal structure, etc.) may be worthwhile.

The hydride formation rate for pure U metal initially exposed to H gas has been measured over a fairly wide range of temperatures and pressures. However, the existing models for the formation rate seem to be lacking in several respects. None of the models are able to accurately reproduce the experimental results over all experimental conditions of interest. Most of the modeling studies that we found in the literature were executed over 20 years ago using rather primitive computation techniques. With this in mind, improvements which enable more accurate modeling are certainly foreseeable with modern computing technology.

Oxide formation on uranium surfaces is a phenomenon which is readily accessible to many common surface techniques. As a result, it is not surprising to us that this aspect of the U+H has been investigated quite thoroughly. Nevertheless, understanding the behavior of oxygen in small hydride particles is an avenue of research which could be of further interest. Chemical reactions with gases other than O_2 , N_2 , and CO_2 have not been studied as extensively. With this in mind, understanding the chemistry of more "exotic" reactions could reveal unforeseen benefits.

To protect against accidental air-ingress, the findings and guidelines presented by Longhurst in Ref. [39] seem to be sufficient from the perspective of designing uranium beds. Other potential failure modes which could lead to rapid tritium release, to our knowledge, have not been investigated as thoroughly, and could be a topic of further study.

X. List of figures

Fig. 1: van't Hoff plots for UH_3 compiled from a number of laboratories. Data from Table 3 of Penzhorn's review [9].

Fig. 2: Pressure-composition isotherms at high hydrogen concentration ($X \approx 3.0$). Data compiled from Libowitz [12].

Fig. 3: Pressure-composition isotherms over a wide range of H/U ratios. Data compiled from Libowitz [12].

Fig. 4: X-ray diffraction scans showing UH_3 and UT_3 aged for 420 days. The UT_3 data indicate substantial lattice distortion, presumably from the formation of ^3He bubbles within the material. (From Ref. [21], used with permission.)

Fig. 5: ^3He retained in metal tritides, as measured by Bowman [17] and Malinowski [22]. The different markers indicate individual samples which were tested.

Fig. 6: Thermal desorption scans obtained by Berezsko et al. [23] which show the release of ^3He and T from uranium samples which had been hydrided with 30% T and 70% D. Measurements obtained with mass spectrometer; all data are for $m/q=3$.

Fig. 7: Thermal desorption scans obtained by Berezsko et al. [23] which show the release of various components ($m/q=3$, $m/q=4$, $m/q=6$) as a function of temperature. In case (a), the uranium sample has been aged 1.6 y after initial tritium exposure, whereas 2.2 y has elapsed in case (b).

Fig. 8: SEM cross-section of a uranium foil (a) before and (b) after exposure to $\text{H}_2(\text{g})$. The reaction interface separating the hydride phase from the α -phase can be clearly seen in panel (b). (Images from Bloch [28], used with permission.)

Fig. 9: SEM images of U foils obtained by Bloch [30] showing initial stage of hydride formation on a U surface. Case (a) shows the virgin material, (b-c) show the pre-induction stage, whereas (d-f) show the linear growth stage. Each sample was heated to 250 °C and exposed to H at a pressure of 900 torr. (Used with permission.)

Fig. 10: A continuation of the SEM images from Bloch [30]. Panel (a) shows the pre-induction stage once again. The linear growth regime for the hydride islands is displayed in (b-c); the islands grow together and induce cracking of the surface, as shown in (d-f). (Used with permission.)

Fig. 11: Hydriding rate data obtained by Powell [26] for a uranium rod using a high speed data acquisition system. The data shown was compiled from a sequence of four hydriding runs, compiled to appear as a single exposure. Prior to the experimental run, the specimens were fabricated from an as-received billet, machined to a 3.18 mm dia., and annealed at 250 °C. (Figure reproduced from Ref. [26], used with permission.)

Fig. 12: Hydride formation rate as a function of exposure pressure, based on uranium sheet data from Powell [26].

Fig. 13: Model proposed by Wang for oxide and hydride layers in uranium.

Fig. 14: Comparison of Auger depth profiles for as-received uranium (a) cleaned with water and solvents, (b) cleaned with 50% HNO_3 and (c) polished electrolytically. Vertical scale indicates AES peak intensities. (Plot from Swissa, Ref. [38], used with permission.)

Fig. 15: Auger depth profiles showing the initial distribution of oxygen on the surface (a) after electrolytic cleaning and prior to thermal annealing and (b) after heating to 600 °C for 40 min. (Plot from Swissa, Ref. [38], used with permission.)

References

1. Dantzer, P., *Metal Hydride Technology: A Critical Review*, in *Topics in Applied Physics: Hydrogen in Metals III - Properties and Applications*, H. Wipf, Editor. 1997, Springer-Verlag: Berlin. p. 279-340.
2. Carlson, R.S. *The Uranium-Tritium System - The Storage of Tritium*. in *Radiation Effects and Tritium Technology for Fusion Reactors*. 1976. Gatlinburg, TN.
3. Longhurst, G.R., et al. *Storage and assay of tritium in STAR*. in *7th International Conference on Tritium Science and Technology*. 2004. Baden Baden, GERMANY: Amer Nuclear Society.
4. Totemeier, T.C., *Characterization of uranium corrosion products involved in a uranium hydride pyrophoric event*. *Journal of Nuclear Materials*, 2000. **278**(2-3): p. 301-311.
5. Hayashi, T., et al. *Safe handling experience of a tritium storage bed*. in *8th International Symposium on Fusion Nuclear Technology*. 2007. Heidelberg, GERMANY: Elsevier Science Sa.
6. Shuai, M., et al., *Hydrogen absorption-desorption properties of UZr0.29 alloy*. *Journal of Nuclear Materials*, 2002. **301**(2-3): p. 203-209.
7. Manchester, F.D., *The H-U (Hydrogen-Uranium) System*. *Journal of Phase Equilibria*, 1995. **16**(3): p. 13.
8. Johnson, Q., T.J. Biel, and H.R. Leider, *ISOTOPIC SHIFTS OF UNIT-CELL CONSTANTS OF ALPHA-TRIHYDRIDES AND BETA-TRIHYDRIDES OF URANIUM - UH₃, UD₃, UT₃*. *Journal of Nuclear Materials*, 1976. **60**(2): p. 231-233.
9. Penzhorn, R.D., M. Devillers, and M. Sirch, *EVALUATION OF ZRCO AND OTHER GETTERS FOR TRITIUM HANDLING AND STORAGE*. *Journal of Nuclear Materials*, 1990. **170**(3): p. 217-231.
10. Mallet, M.W. and M.J. Trzeciak, *Hydrogen-Uranium Relationships*. *Trans. ASM*, 1958. **50**: p. 981-989.
11. Tanabe, T., S. Miura, and S. Imoto, *ISOTOPE EFFECT IN DISSOCIATION OF URANIUM HYDRIDE*. *Journal of Nuclear Science and Technology*, 1979. **16**(9): p. 690-696.
12. Libowitz, G.G. and T.R.P. Gibb, *HIGH PRESSURE DISSOCIATION STUDIES OF THE URANIUM HYDROGEN SYSTEM*. *Journal of Physical Chemistry*, 1957. **61**(6): p. 793-795.
13. Abraham, B.M. and H.E. Flotow, *THE HEATS OF FORMATION OF URANIUM HYDRIDE, URANIUM DEUTERIDE AND URANIUM TRITIDE AT 25-DEGREES*. *Journal of the American Chemical Society*, 1955. **77**(6): p. 1446-1448.
14. Costantino, M.S., J.F. Lakner, and R. Bastasz, *SYNTHESIS OF MONOLITHIC URANIUM HYDRIDE AND URANIUM DEUTERIDE*. *Journal of the Less-Common Metals*, 1990. **159**(1-2): p. 97-108.
15. Swift, D., *The thermal conductivity of spherical metal powders including the effect of an oxide coating*. *Int. J. Heat Mass Transfer*, 1966. **9**: p. 1061-1074.
16. Erickson, K.L., Roth E.P., and Lakner, J.F., *Thermophysical Properties of Uranium Hydride*. *Sandia Report*, 1983. **SAND83-1531A**.
17. Bowman, R.C. and A. Attalla, *NMR studies of the helium distribution in uranium tritide*. *PHYSICAL REVIEW B*, 1977. **16**(5): p. 1828.

18. Bowman, R.C.J., *Distribution of Helium in Metal Tritides*. *Nature*, 1978. **271**: p. 531-533.
19. Cowgill, D.F. and R.E. Norberg, *SPIN-LATTICE RELAXATION AND CHEMICAL-SHIFT OF KR-83 IN SOLID AND LIQUID KRYPTON*. *PHYSICAL REVIEW B*, 1973. **8**(11): p. 4966-4974.
20. Barash, Y.B., J. Barak, and M.H. Mintz, *NMR-STUDY OF HYDROGEN IN FERROMAGNETIC BETA-UH3*. *PHYSICAL REVIEW B*, 1984. **29**(11): p. 6096-6104.
21. Ao, B.Y., et al., *X-ray diffraction analysis of uranium tritide after aging for 420 days*. *Journal of Nuclear Materials*, 2009. **384**(3): p. 311-314.
22. Malinowski, M.E. and P.R. Coronado. *Helium Release from Uranium Tritide*. in *Radiation Effects and Tritium Technology for Fusion Reactors*. 1975. Gatlinburg, TN.
23. Berezhko, P.G., et al., *Radiogenic helium thermodesorption from uranium deuterotritide*. *Fusion Technology*, 1996: p. 1281-1284.
24. Ensinger, W. and H.R. Muller, *THE ROTATING WING DRUM - AN APPARATUS FOR ION-BEAM TREATMENT OF POWDERS*. *Review of Scientific Instruments*, 1994. **65**(9): p. 2963-2967.
25. Cowgill, D.F. *Helium nano-bubble evolution in aging metal tritides*. in *7th International Conference on Tritium Science and Technology*. 2004. Baden Baden, GERMANY: Amer Nuclear Society.
26. Powell, G.L., W.L. Harper, and J.R. Kirkpatrick. *THE KINETICS OF THE HYDRIDING OF URANIUM METAL*. in *International Symp on Metal-Hydrogen Systems, Fundamentals and Applications*. 1990. Banff, Canada: Elsevier Science Sa Lausanne.
27. Kirkpatrick, J.R. and J.B. Condon. *THE LINEAR SOLUTION FOR HYDRIDING OF URANIUM*. in *International Symp on Metal-Hydrogen Systems, Fundamentals and Applications*. 1990. Banff, Canada: Elsevier Science Sa Lausanne.
28. Bloch, J. and M.H. Mintz, *Kinetics and mechanism of the U-H reaction*. *Journal Of The Less Common Metals*, 1981. **81**(2): p. 301-320.
29. Wicke, E. and K. Otto, *Z. Phys. Chem.*, 1962. **31**(1962).
30. Bloch, J., et al., *THE INITIAL KINETICS OF URANIUM HYDRIDE FORMATION STUDIED BY A HOT-STAGE MICROSCOPE TECHNIQUE*. *Journal of the Less-Common Metals*, 1984. **103**(1): p. 163-171.
31. Bloch, J. and M.H. Mintz, *The effect of thermal annealing on the hydriding kinetics of uranium*. *Journal Of The Less Common Metals*, 1990. **166**(2): p. 241-251.
32. Condon, J.B. and E.A. Larson, *KINETICS OF URANIUM-HYDROGEN SYSTEM*. *Journal of Chemical Physics*, 1973. **59**(2): p. 855-865.
33. Condon, J.B., *CALCULATED VS EXPERIMENTAL HYDROGEN REACTION-RATES WITH URANIUM*. *Journal of Physical Chemistry*, 1975. **79**(4): p. 392-397.
34. Lindner, D.L., *ISOTHERMAL DECOMPOSITION OF URANIUM HYDRIDE*. *Journal of the Less-Common Metals*, 1990. **157**(1): p. 139-146.
35. Bloch, J., et al., *Surface spectroscopy studies of the oxidation behavior of uranium*. *Journal of Nuclear Materials*, 1982. **105**(2-3): p. 196-200.

36. Wang, X.L., X.G. Fu, and Z.P. Zhao. *Surface chemical behavior of uranium metal in hydrogen atmosphere studied by XPS. in 7th International Conference on the Structure of Surfaces. 2002. Newcastle, Australia: World Scientific Publ Co Pte Ltd.*
37. Balooch, M. and A.V. Hamza, *Hydrogen and water vapor adsorption on and reaction with uranium. Journal of Nuclear Materials, 1996. 230(3): p. 259-270.*
38. Swissa, E., et al., *Heat-induced redistribution of surface oxide in uranium. Journal of Nuclear Materials, 1990. 173(1): p. 87-97.*
39. Longhurst, G.R., et al., *Experimental evaluation of the consequences of uranium bed air-ingress accidents. Fusion Technology, 1992. 21.*
40. Luo, W.F., et al., *Equilibrium isotope effects in the preparation and isothermal decomposition of ternary hydrides Pd(HxD1-x)(y) (0 < x < 1 and y > 0.6). Journal of Physical Chemistry B, 2008. 112(27): p. 8099-8105.*

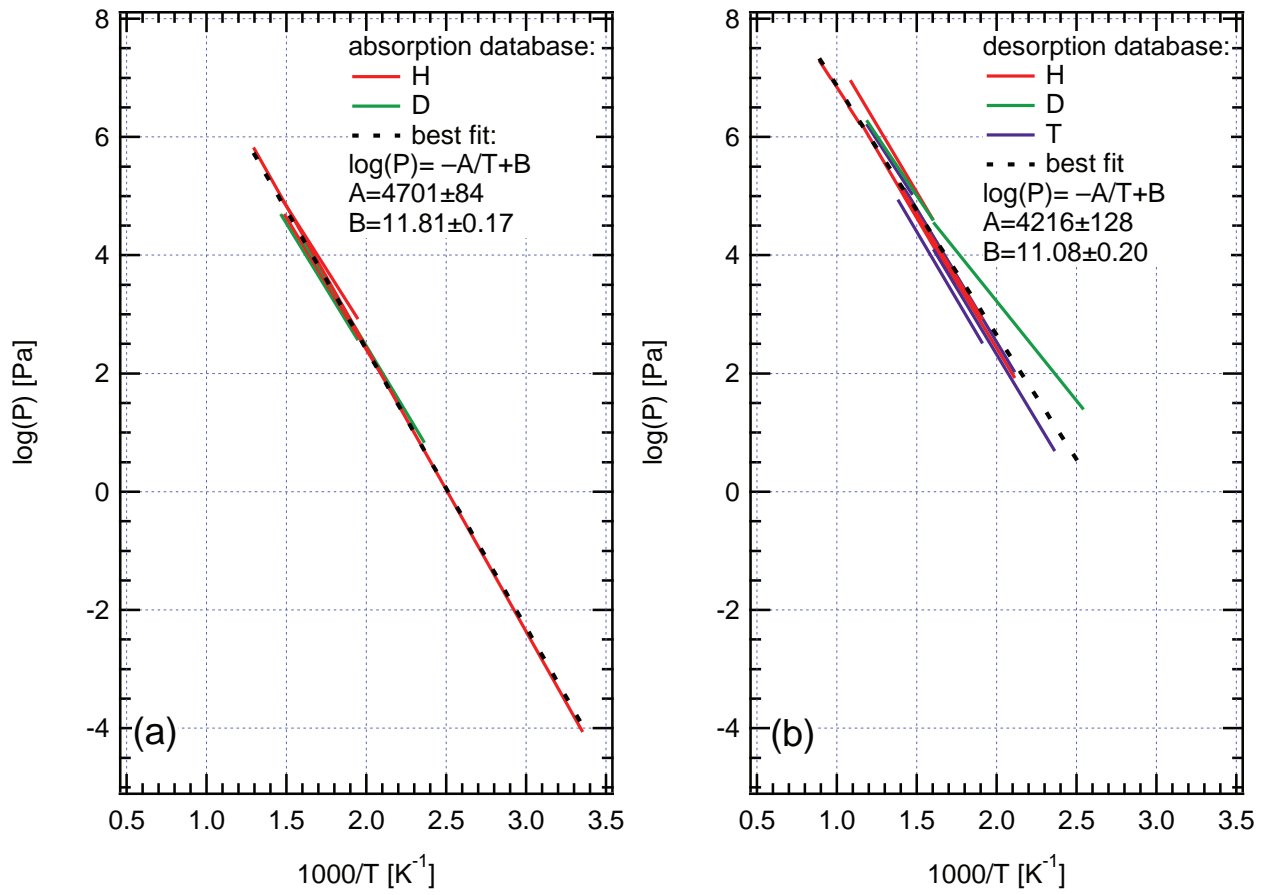


Fig. 1

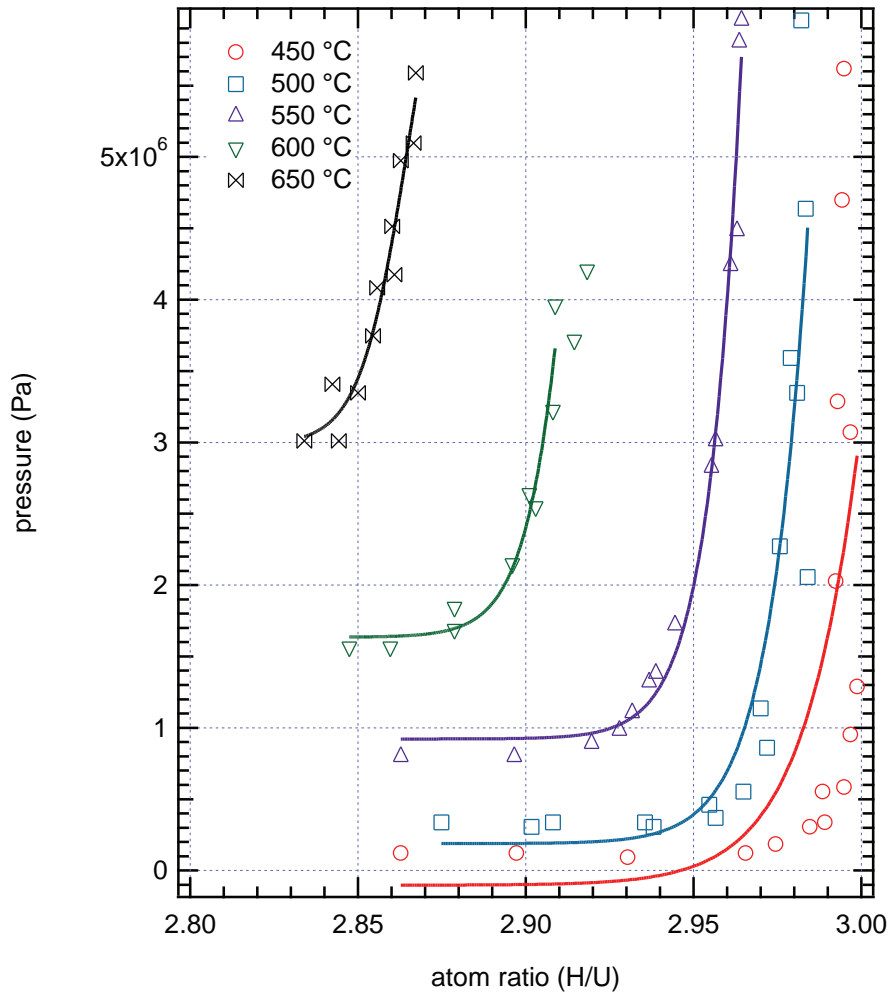


Fig. 2

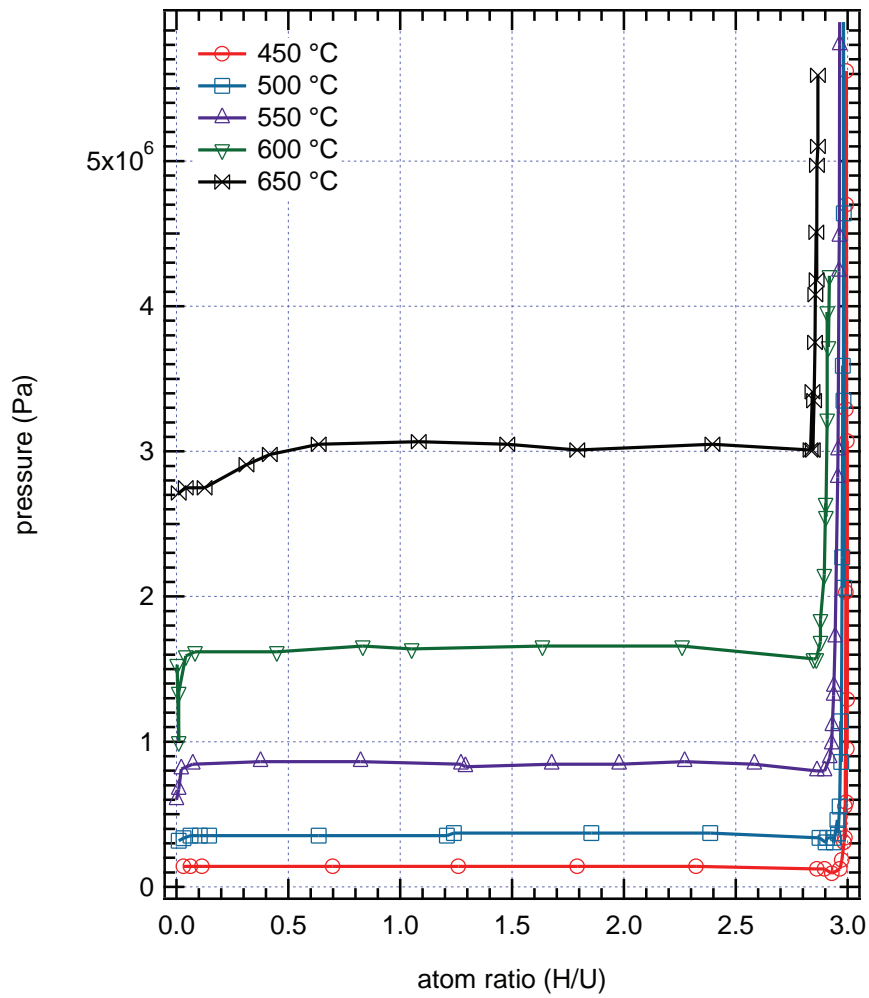


Fig. 3

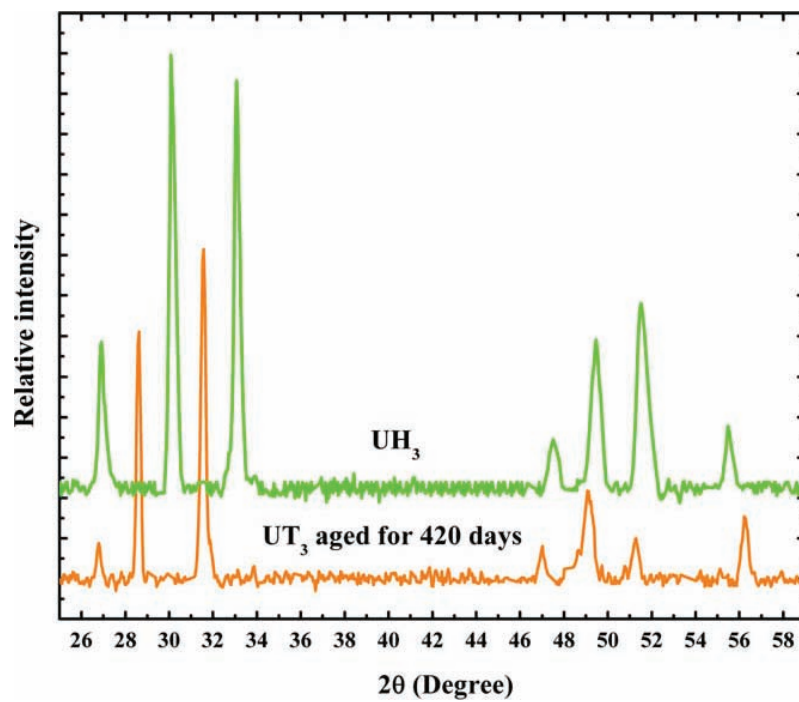


Fig. 4

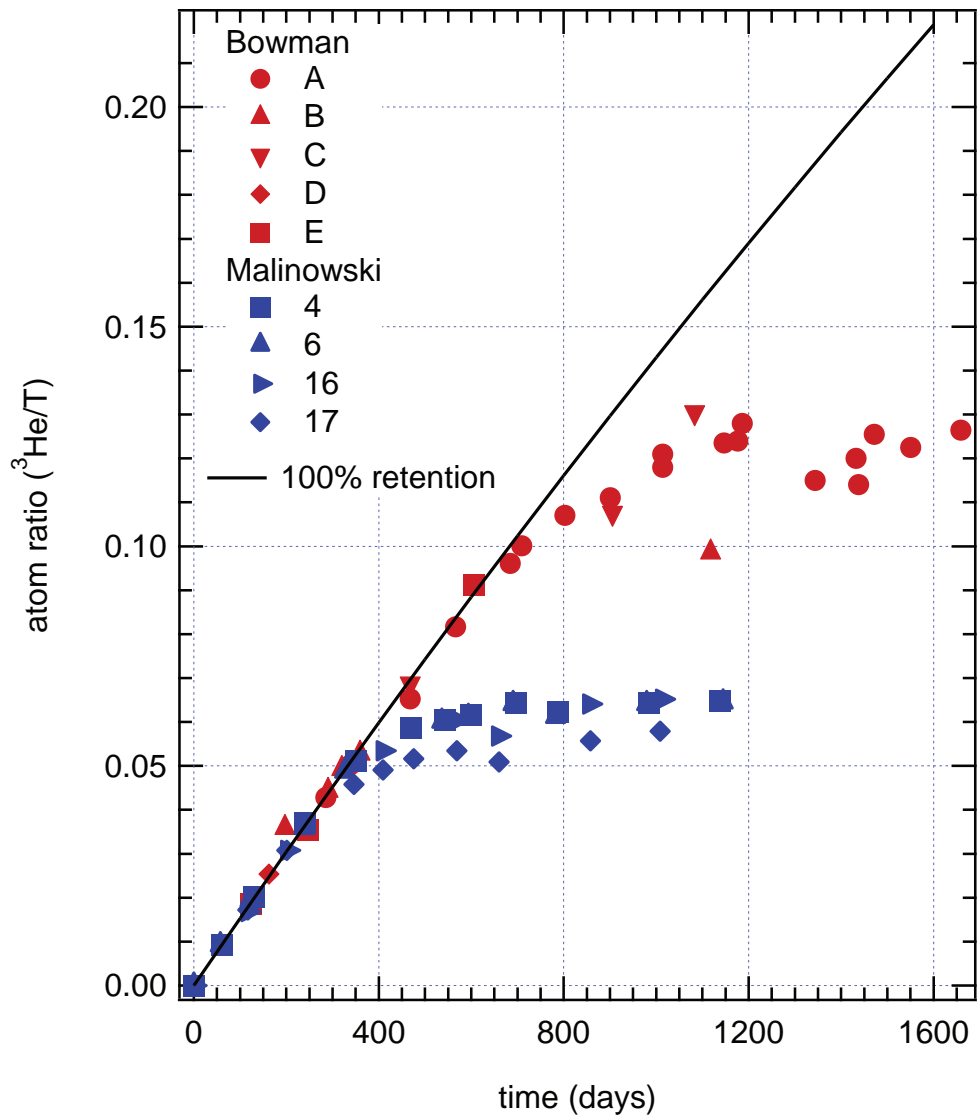


Fig. 5

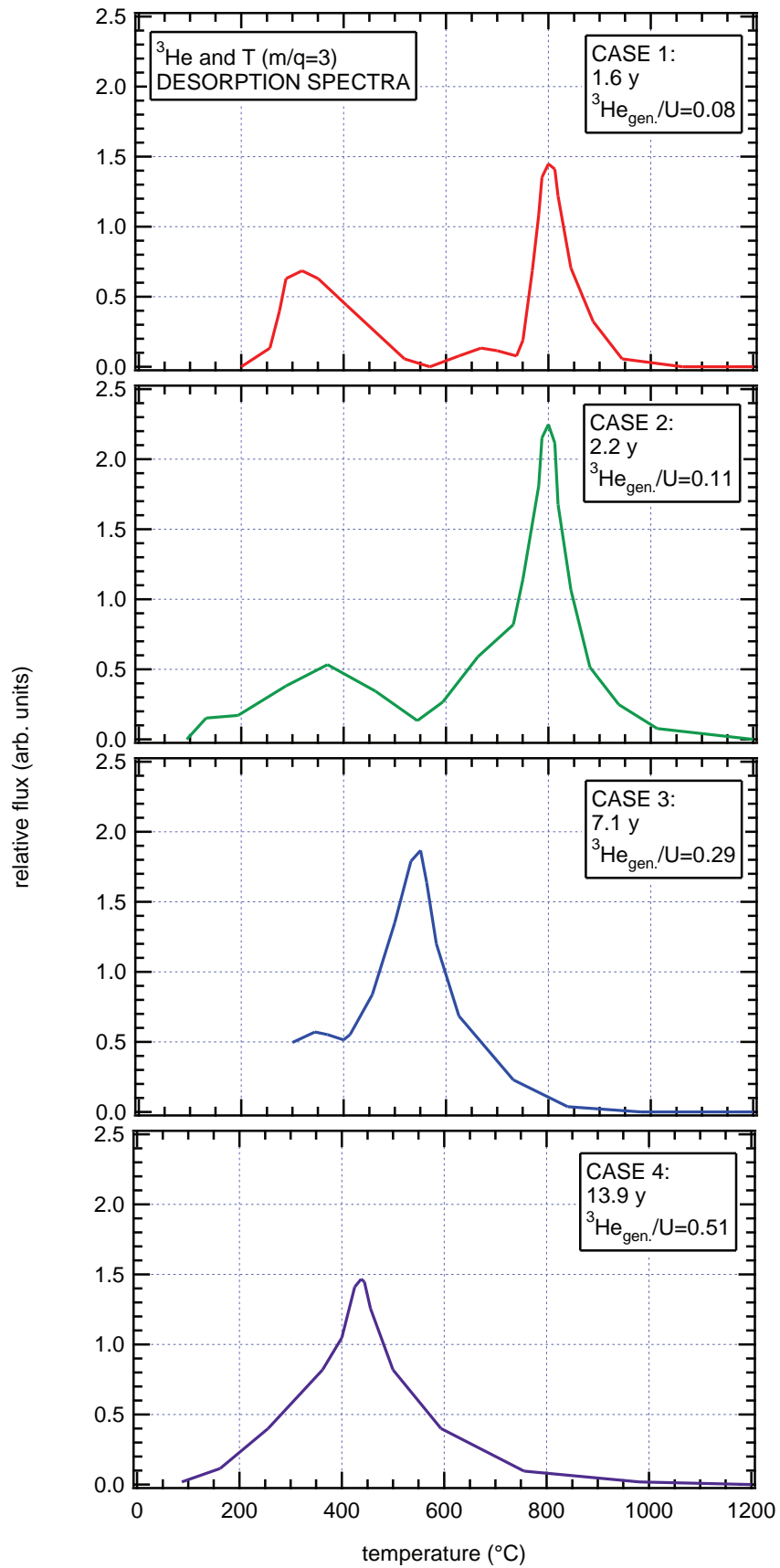


Fig. 6

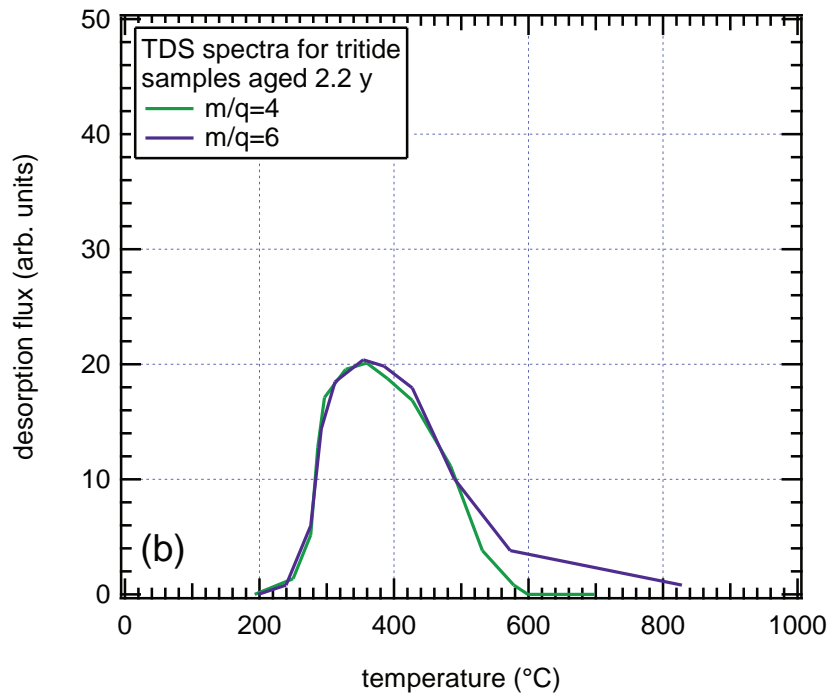
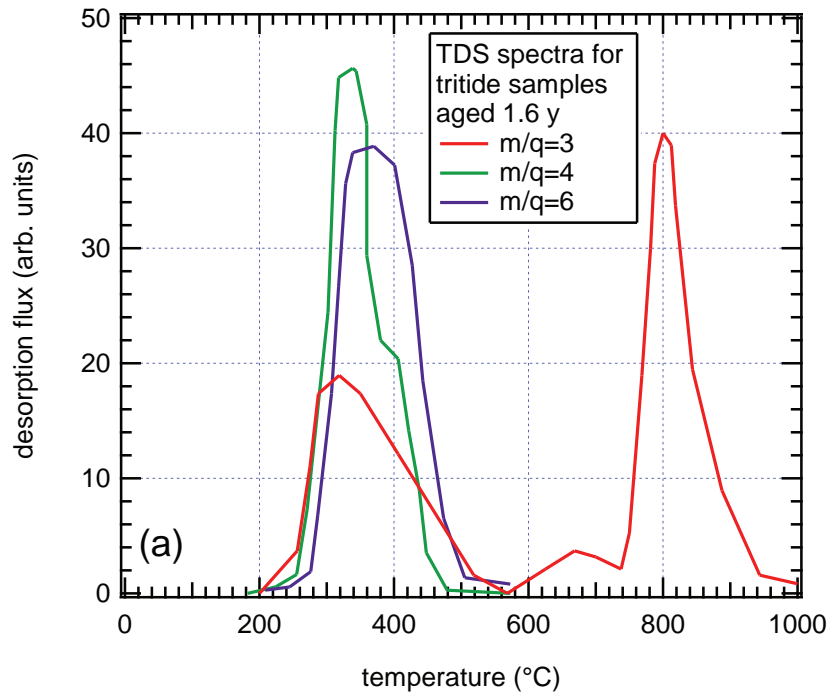


Fig. 7

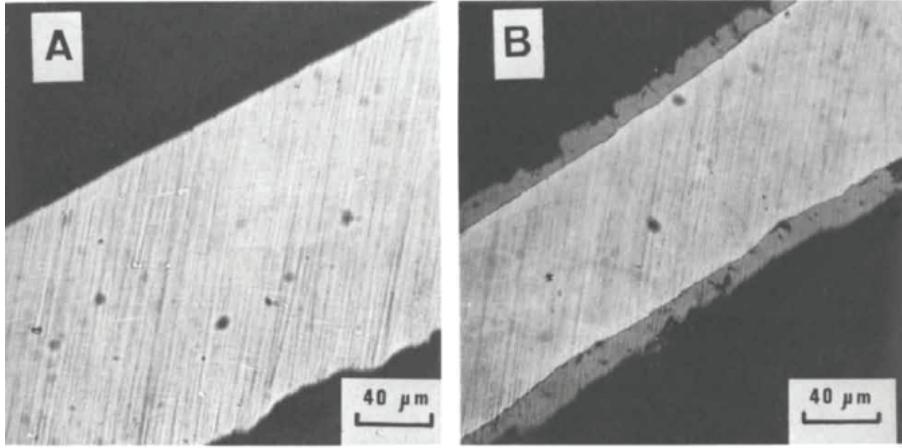


Fig. 8

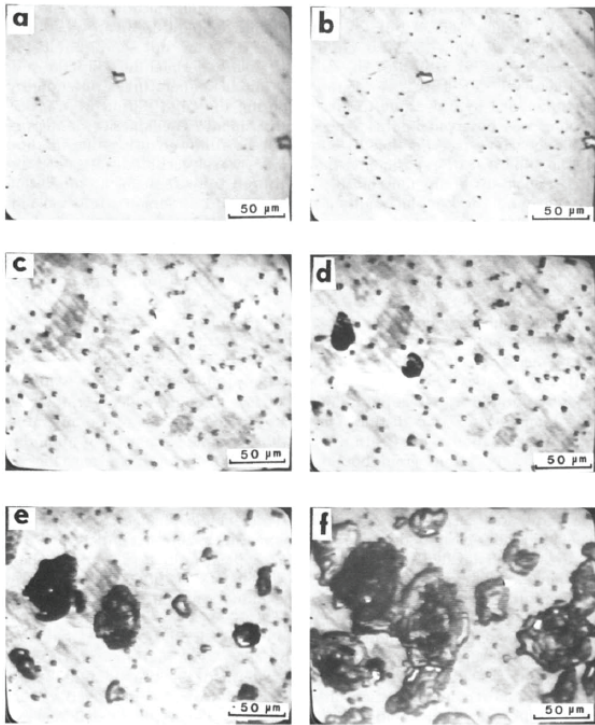


Fig. 9

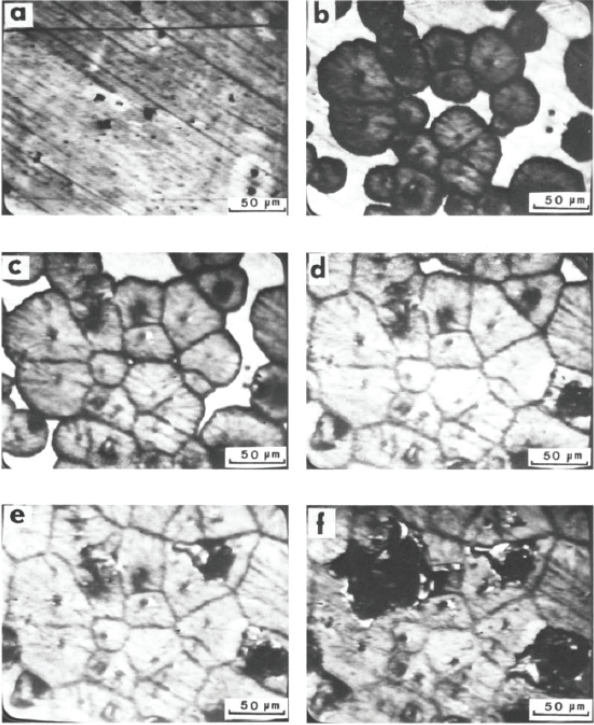


Fig. 10

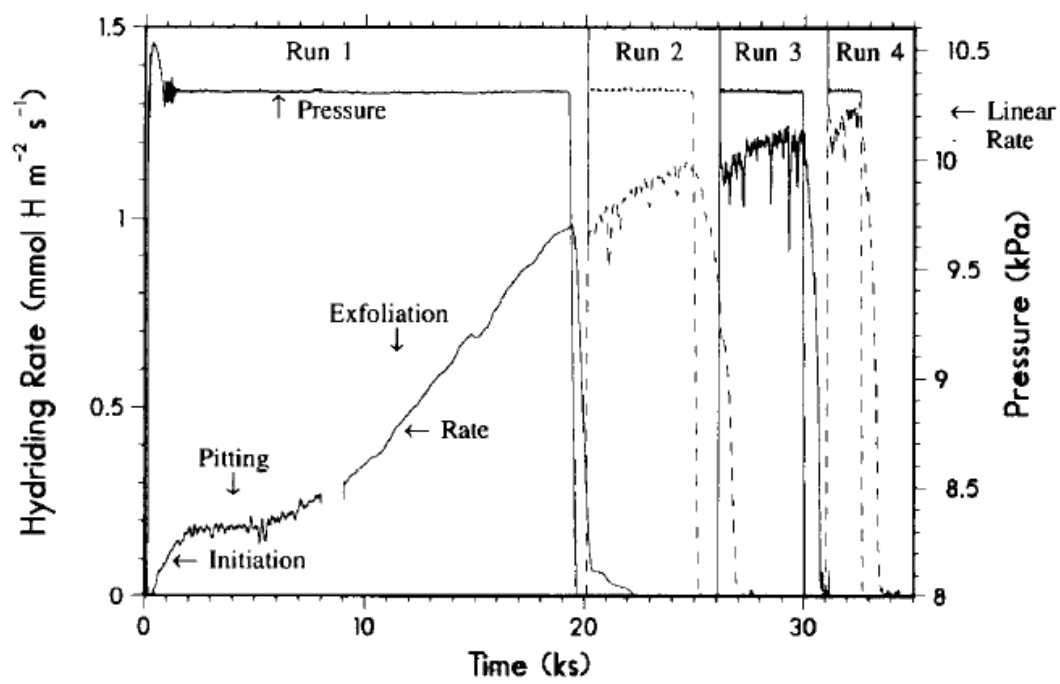


Fig. 11

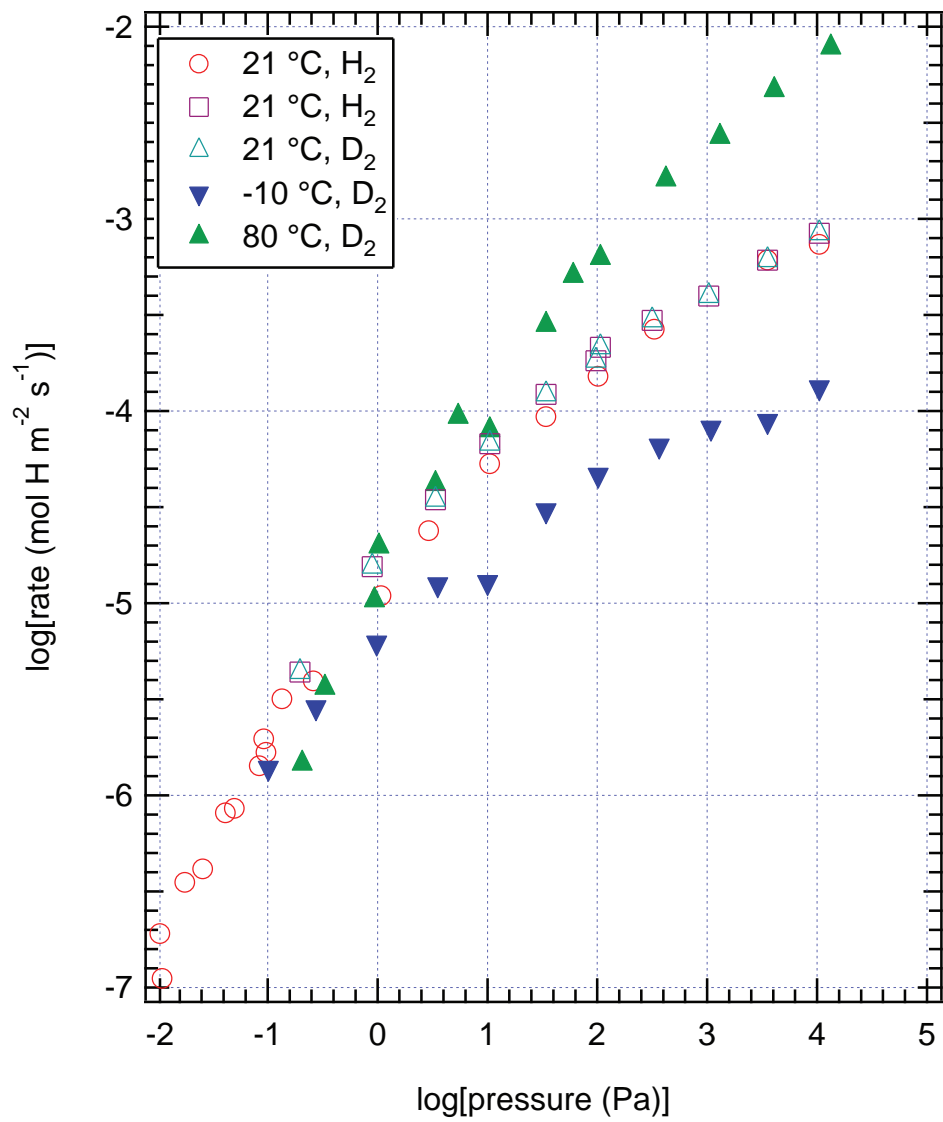


Fig. 12



Fig. 13

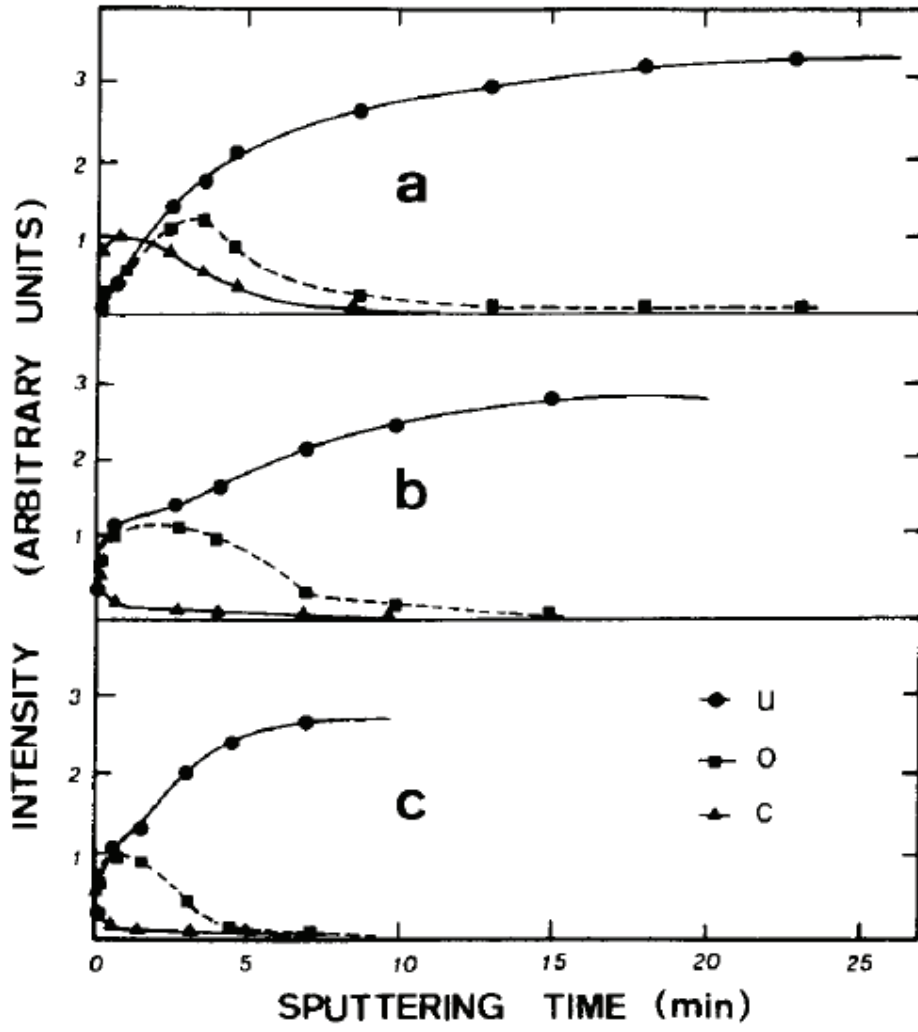


Fig. 14

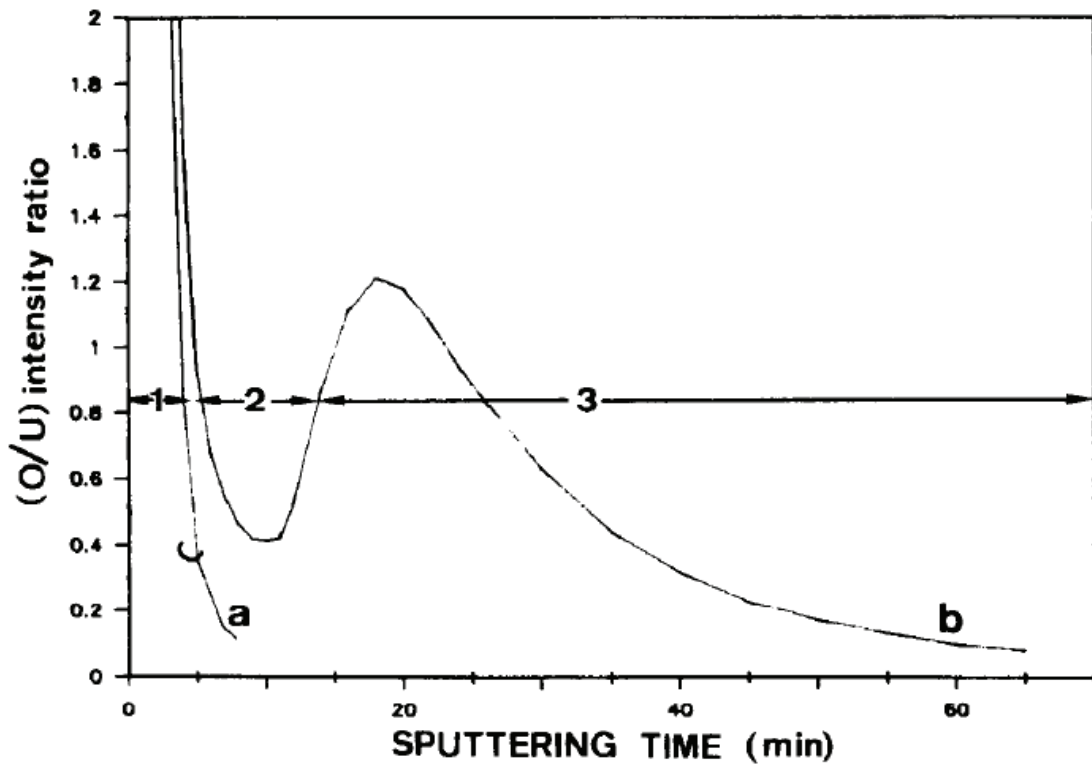


Fig. 15



Sandia National Laboratories